Synthesis of the bulky *m*-terphenyl phenol Ar*OH (Ar* = C_6H_3-2,6-Mes_2, Mes = 2,4,6-trimethylphenyl) and the preparation and structural characterization of several of its metal complexes

Diane A. Dickie, Ian S. MacIntosh, Daisuke D. Ino, Qi He, Ojisamola A. Labeodan, Michael C. Jennings, Gabriele Schatte, Charles J. Walsby, and Jason A.C. Clyburne

Abstract: The bulky *m*-terphenyl phenol Ar*OH **1** (Ar* = C_6H_3-2,6-Mes_2, Mes = 2,4,6-trimethylphenyl) was synthesized via the treatment of Ar*Li with nitrobenzene. The phenol **1** is prepared in modest to good yield using this method. Attempts were also made to prepare **1** through oxidation of the bulky boronic acid Ar*$B(OH)_2$ with Oxone®, but this reaction was not suitable for preparative-scale reactions. Side products of the reaction between Ar*Li and nitrobenzene were identified as Ar*[N(O)Ph] and $[C_6H_5N(O)]_2$ and were characterized by X-ray crystallography and EPR spectroscopy. A variety of main-group and transition-metal complexes of Ar*OH were prepared, namely $Sn(OAr^*)_2$, $Ge(OAr^*)_2$, $[N(SiMe_3)_2]Ge(OAr^*)$, $[Me_2Al(OAr^*)]_2$, and $Ti(NMe_2)(OAr^*)_2$. All compounds were characterized spectroscopically and most were studied by single-crystal X-ray diffraction as well.

Key words: *m*-terphenyl, main-group compounds, X-ray crystallography, multinuclear NMR spectroscopy, EPR spectroscopy.

Résumé : On a réalisé la synthèse du *m*-terphénylphénol encombré, Ar*OH, **1**, (Ar* = C_6H_3-2,3-Mes_2; Mes = 2,4,6-triméthylphényle) en faisant réagir du Ar*Li avec du nitrobenzène. Avec cette méthode, on obtient le phénol **1** avec des rendements allant de modestes à bon. On a aussi tenté de préparer le phénol **1** en procédant à l’oxydation de l’acide boronique encombré Ar*$B(OH)_2$ avec de l’Oxone®, mais cette réaction n’est pas appropriée pour des réactions à l’échelle préparative. On a identifié des sous-produits de la réaction entre le Ar*Li et le nitrobenzène, dont le Ar*[N(O)Ph] et le $[C_6H_5N(O)]$ et on a procédé à leur identification par diffraction des rayons X et par spectroscopie RPE. On a préparé une variété de complexes du Ar*OH avec des métaux de transition et du groupe principal, dont $Sn(OAr^*)_2$, $Ge(OAr^*)_2$, $[N(SiMe_3)_2]Ge(OAr^*)$, $[Me_2Al(OAr^*)]_2$ et $Ti(NMe_2)(OAr^*)_2$. On a caractérisé tous les composés par spectroscopie et la plupart de ces composés ont été étudiés par diffraction des rayons X de cristaux uniques.

Mots-clés : *m*-terphényle, composés du groupe principal, diffraction des rayons X, spectroscopie RMN multinucléaire, spectroscopie RPE.

[Traduit par la Rédaction]

Introduction

The ability to control the coordination environment around a metal is perhaps the most important factor in controlling its reactivity. This is often achieved with the use of sterically demanding ligands. Perhaps the most common class of bulky substituents currently in use are *m*-terphenyls (1), molecules with two aryl substituents arranged *meta* to one another on a central phenyl ring. As shown in Fig. 1, the aryl groups twist out of the plane of the central ring to form a bowl-shaped pocket with a diameter of approximately 12 Å. This pocket acts as a steric shield for reactive species found within it. The steric protection provided by the *m*-terphenyl can be tuned by varying the nature of the aryl

Received 5 July 2007. Accepted 19 October 2007. Published on the NRC Research Press Web site at canjchem.nrc.ca on 7 December 2008.

D.A. Dickie, D.D. Ino, Q. He, O.A. Labeodan, and C.J. Walsby. Department of Chemistry, Simon Fraser University, Burnaby, BC V5A 1S6, Canada.
I.S. MacIntosh, and J.A.C. Clyburne.[1] Department of Chemistry, Saint Mary’s University, Halifax, NS B3H 3C3, Canada.
M.C. Jennings. Department of Chemistry, The University of Western Ontario, London, ON N6A 5B7, Canada.
G. Schatte. Saskatchewan Structural Sciences Centre, University of Saskatchewan, Saskatoon, SK S7N 5C9, Canada.

[1] Corresponding author: (email: jason.clyburne@smu.ca).

doi:10.1139/V07-131

Fig. 1. The pocket formed by the *m*-terphenyl 2,6-bis(2,4,6-trimethylphenyl)benzene is shown in the space-filling diagram.

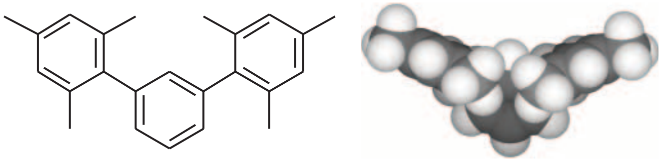

Fig. 2. Selected *m*-terphenyl phenols, from least to most bulky.

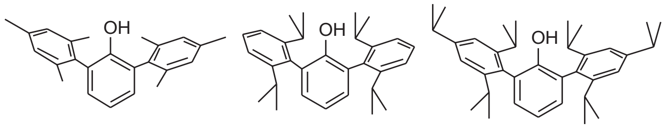

1 **2** (11) **3** (11)

Scheme 1. Synthesis of boronic acids **4** and **5**.

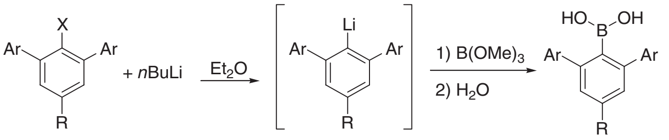

X = Br, Ar = Ph, R = Ph **4**
X = I, Ar = Mes, R = Ph **5**

substituents. Common groups include phenyl, 2,4,6-trimethylphenyl (mesityl, Mes), 2,6-diisopropylphenyl (Dipp), and 2,4,6-triisopropylphenyl (Trip).

During the past several years, we have been interested in the coordination chemistry of "substituted" *m*-terphenyl ligands. These studies have resulted in the isolation of unusual coordination geometries for amidinates (2) and carboxylates (3), and here we continue with an examination of phenoxide chemistry. Alkoxides and aryloxides are among the most versatile ligands known and have been placed on virtually every element of the periodic table (4). It is not surprising, therefore, that one of the very first substituted *m*-terphenyls to be used as a ligand was 2,6-diphenylphenol, in a tungsten complex that was subsequently used as an olefin metathesis catalyst (5). Rothwell (6) and others (7) have since explored the structure and reactivity, including catalytic behavior, of many other early transition-metal complexes of this ligand.

The search for new and improved catalysts has also motivated much of the research into main-group *m*-terphenyl phenol complexes (8), based largely on the pioneering work by Yamamoto and co-workers on aluminium tris(2,6-diphenylphenoxide) (9). This molecule and related complexes have served as useful catalysts for stereoselective Claisen rearrangements as well as conjugate addition to α,β-unsaturated carbonyl compounds, and *exo*-selective Diels–Alder additions (opposite to the typical *endo* preference) (10).

Key to the successful use of these bulky complexes is a simple preparation of the ligands. Whereas some bulky phenols, such as 2,6-diphenylphenol, are commercially available, most others are not. Since steric bulk often dominates or governs the chemistry observed for the complexes, a convenient route into these molecules is desirable. We note here that recent reports by the research group of Power and co-workers described the preparation of bulky phenols **2** and **3** (11) (Fig. 2). Our work aims to complement these studies.

Results and discussion

Ligand synthesis

The targeted *m*-terphenyl phenol for this study was 2,6-bis(2,4,6-trimethylphenyl)phenol, Ar*OH **1**, which had previously only been synthesized as a by-product in the reaction of the corresponding *m*-terphenyl copper complex with oxygen (12), or through the palladium-catalyzed cross coupling of phenol with 2,4,6-trimethylbromobenzene (13). Neither of these routes involved the *m*-terphenyl precursors that were readily available, namely Ar*I or a convenient metallated derivative, so two alternative routes were developed.

One proposed route involved the oxidation of *m*-terphenyl boronic acids with Oxone® (14). Lithiation of either 2,4,6-triphenylbromobenzene or 2,6-bis(2,4,6-trimethylphenyl)iodobenzene (Ar*I) in diethyl ether, followed by addition of trimethylborate and aqueous work-up gave the *m*-terphenyl boronic acids **4** and **5**, respectively (Scheme 1). NMR spectroscopy was used to characterize the boronic acids **4** and **5**. The most definitive signal was the two-proton singlet at 4.11 or 4.06 ppm in the spectra of **4** and **5**, respectively, assigned to the $–B(OH)_2$ protons. The upfield shift of these protons relative to phenylboronic acid (4.61 ppm) (15) may be due to shielding by the aryl substituents. The ^{11}B NMR spectra of **4** and **5** each showed a single sharp peak, at 31.4 ppm for **4** and 29.3 ppm for **5**. These values are comparable to other phenylboronic acids (16).

Although these compounds were initially prepared as starting materials for the *m*-terphenyl phenol synthesis, somewhat surprising differences in the O–H absorption region in the IR spectra of **4** and **5** prompted us to more closely examine their intrinsic properties before proceeding further. In the triphenyl-substituted derivative **4**, there was a very strong O–H stretch at 3586 cm^{-1} and a broad absorption at 3280 cm^{-1}, while **5** showed instead four weak absorptions between 3668 and 3417 cm^{-1}. Since this region is primarily affected by hydrogen bonding interactions, attempts were made to grow crystals of both new *m*-terphenyl boronic acids to see if they exhibited different intermolecular interactions. Unfortunately, only **5** yielded crystals suitable for single crystal X-ray diffraction (Fig. 3).

The X-ray crystallographic analysis revealed that, as expected, there is intermolecular [O–H···O] hydrogen bonding in **5**, with O(2) as the donor and O(1) as the acceptor, forming a zigzag chain (Fig. 4). In the absence of other hydrogen bond donor/acceptor groups, all other structurally characterized (17) phenylboronic acid derivatives form homodimers with eight-membered $B_2O_4H_2$ rings rather than infinite chains like **5**. Similar head-to-head homo-dimerization was also observed in two related *m*-terphenyl substituted carboxylic acids (18). Since the carboxylic acids both feature smaller aryl substituents than **5** (phenyl vs. 2,4,6-trimethylphenyl), **4**, which also has the smaller phenyl substituents, may also form a homo-dimer, and that would explain the differences in the IR spectra of **4** and **5**.

Once the boronic acids **4** and **5** were in hand, reactions to oxidize them to the respective *m*-terphenyl phenols were performed using Oxone® in basic solution (14). This reac-

Fig. 3. Molecular structure of 2,6-bis(2,4,6-trimethylphenyl)phenylboronic acid **5**. Thermal ellipsoids are shown at 50% probability, and hydrogen atoms, except OH protons, have been removed for clarity. Selected bond lengths (Å) and angles (°): B(1)—O(1A) 1.603(18); B(1)— O(2A) 1.212(12); B(1)—C(1) 1.552(8); O(1A)–B(1)–O(2A) 112.9(9).

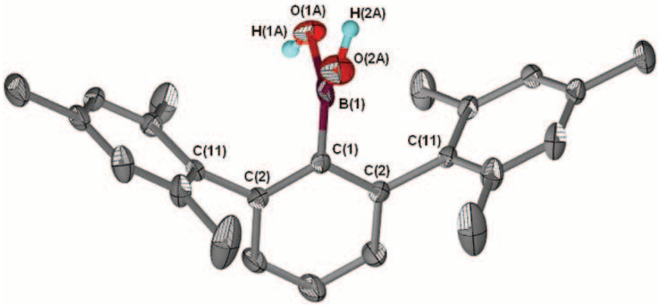

Scheme 2. Synthesis of *m*-terphenyl phenol **1** and nitrosobenzene complex **6**.

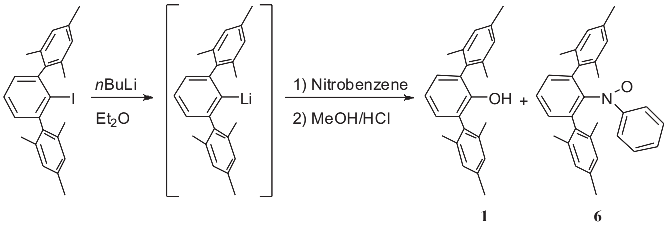

tion produces very low yield (trace) of the desired bulky phenols, and hence work in this area was stopped and a new route was sought.

Generation of bulky phenols from Ar*Li and nitrobenzene

During the course of our boronic acid experiments, Power and co-workers (11) developed a synthesis of bulkier *m*-terphenyl phenols, namely **2** and **3**, directly from the lithiated intermediate Ar*Li, so this more direct and higher yielding route was pursued. Lithiation of Ar*I with *n*-butyllithium in ethereal solution followed by addition of excess nitrobenzene at –78 °C results in the immediate formation of a dark red solution that is quenched with methanol to give **1** (Scheme 2).

In the ^{1}H NMR spectrum of the *m*-terphenyl phenol **1**, the O*H* appears as a singlet at 4.53 ppm. The methyl groups are found at 2.33 (*para*) and 2.06 (*ortho*) ppm. Additional evidence for the presence of the OH was provided by strong IR absorptions at 3486 and 3451 cm^{-1}. These stretches are comparable to those reported by Lüning and co-workers (19) for 2,6-bis(2,6-dimethylphenyl)phenol, at 3482 and 3431 cm^{-1}. Four other previously published *m*-terphenyl phenols, namely 2,6-diphenylphenol (20), 2,6-bis(3,5-dimethylphenyl)phenol (19), 2,6-bis(2,6-diisopropylphenyl)phenol **2** (11), and 2,6-bis(2,4,6-triisopropylphenyl)phenol **3** (11), each reported only a single OH stretch between 3520–3533 cm^{-1} in the IR spectrum. Since three of these five compounds had been crystallographically characterized, single-crystal X-ray diffraction studies were performed on **1** to see if there was a difference in hydrogen bonding that could explain the differences in the IR spectra.

Fig. 4. [O–H···O] hydrogen bonds in **5**, viewed along the crystallographic *a* axis.

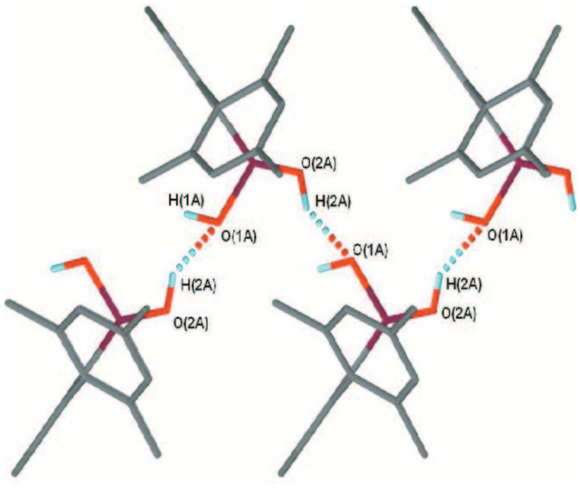

Fig. 5. Molecular structure of 2,6-bis(2,4,6-trimethylphenyl)phenol **1**. Thermal ellipsoids are shown at 50% probability, and all hydrogens, except phenolic protons, have been removed for clarity. Selected bond lengths (Å) and angles (°): O(1)—C(2) 1.356(3); O(31)—C(32) 1.375(3); O(1)–C(2)–C(7) 116.7(2); O(1)–C(2)–C(3) 121.7(2); O(31)–C(32)–C(37) 116.3(2); O(31)–C(32)–C(33) 121.0(2). Hydrogen-bond lengths (Å) and angles (°): O(1)···O(31) 2.823(3); O(1)–H(1A)···O(31) 152.9.

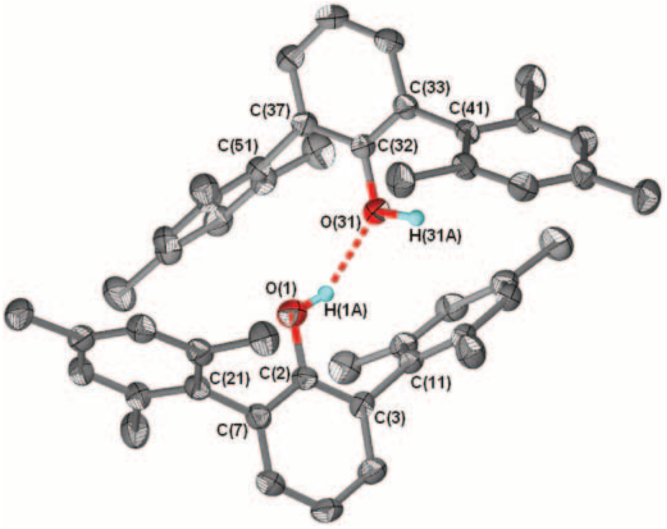

The crystallographic studies revealed that in the solid state, **1** exists as two crystallographically distinct molecules (Fig. 5). These molecules are connected by a weak [O–H···O] hydrogen bond to form a dimer. This is in contrast to the unsubstituted phenol (C_6H_5OH), which forms infinite hydrogen-bonded chains (21) with an average [O···O] distance of 2.67 Å, compared with 2.823(3) Å in **1**. It is also in contrast to all three previously structurally characterized *m*-terphenyl phenols, none of which exhibits [O–H···O] hydrogen bonds. Based on the IR evidence, it would appear that Lüning's 2,6-bis(2,6-dimethylphenyl)phenol follows the

Fig. 6. Molecular structure of nitrosobenzene complex **6** that was isolated as a co-crystal with $[C_6H_5N(O)]_2$, the dimer of nitrosobenzene. Thermal ellipsoids are shown at 50% probability, and hydrogen atoms have been removed for clarity. Selected bond lengths (Å) and angles (°):N(1)—O(1) 1.290(2); N(1)—C(1) 1.443(3); N(1)—C(31) 1.406(3); N(2)—N(2)* 1.128(6); N(2)—O(2) 1.301(5); N(2)—C(41) 1.564(5); O(1)–N(1)–C(1) 116.86(18); O(1)–N(1)–C(31) 119.32(17); C(1)–N(1)–C(31) 123.82(18).

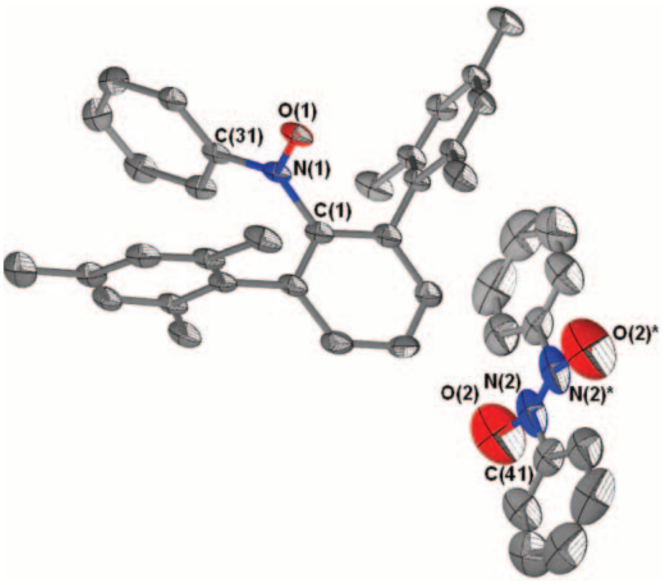

Fig. 7. Main panel: Experimental (top) and simulated (bottom) EPR spectra of nitrosobenzene complex **6** dissolved in CH_2Cl_2. Experimental parameters: ν = 9.86 GHz, microwave attenuation = 20 dB, scan time = 21 s, time constant = 10.24 ms, modulation amplitude = 0.0125 mT, receiver gain = 2.5 × 10^3, average of 17 scans. Simulation parameters: $a(^{14}N)$ = 1.024 mT; $a(^1H \times 3)$ = 0.247 mT; $a(^1H \times 2)$ = 0.088 mT, $a(^1H \times 3)$ = 0.054 mT, linewidth = 0.047 mT. Inset: EPR spectrum of single co-crystal of nitrosobenzene complex **6** with $[C_6H_5N(O)]_2$. Experimental parameters: ν = 9.86 GHz, microwave attenuation = 25 dB, scan time = 21 s, time constant = 10.24 ms, modulation amplitude = 0.01 mT, receiver gain = 6.3 × 10^3, 1 scan.

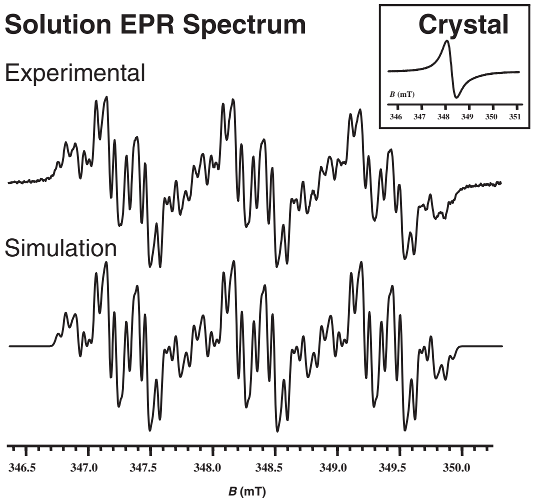

same pattern as **1**, while his 3,5-derivative is more similar to the others (11, 20).

Another feature that was found in each of the crystallographically characterized *m*-terphenyl phenols, including **1**, is an intramolecular [O–H···π] interaction. In the case of the extremely bulky 2,6-bis(2,4,6-triisopropylphenyl)phenol and 2,6-bis(2,6-diisopropylphenyl)phenol, steric hindrance hampers intermolecular [O–H···O] interactions, but does not prevent intramolecular [O–H···π] interactions with a flanking aryl. This interaction occurs primarily through the *ipso* carbon atoms (H···C_{ipso} = 2.64 and 2.39 Å, respectively) (11). In fact, the restricted rotation caused by the presence of such bulky groups may even enhance the interaction by locking the aryls into place.

Restricted rotation is clearly not necessary though, since the crystal structure of the least hindered *m*-terphenyl, 2,6-diphenylphenol, also showed an [O–H···π] interaction of 2.43 Å (20). The corresponding H···C_{ipso} distances in **1** are 2.41 and 2.47 Å [H(1A)···C(11) and H(31A)···C(41), respectively]. It is not immediately clear why 2,6-diphenylphenol does not also engage in [O–H···O] hydrogen bonds like **1**, but it may be that [C–H···π] interactions through the *para* hydrogen of the central phenyl provide more favorable packing interactions. Taken together, these examples illustrate how subtle changes in steric demands can have a large effect on intermolecular interactions.

During the work-up and recrystallization of **1**, a small amount of a highly colored red by-product was also isolated. We performed spectroscopic studies on the red material, and found that NMR studies were not informative because of extensive line broadening, and the IR studies indicated the presence of both aromatic C–H and alkyl C–H fragments, as well as peaks that were tentatively assigned to N–O bonds.

To unambiguously assign the structure, a crystallographic study was performed on the block-shaped crystals (Fig. 6). The results of these studies indicate that the *m*-terphenyl nitrosobenzene addition complex **6** was formed and co-crystallized with homodimerized nitrosobenzene, the other by-product of the phenol synthesis. The formation of the *m*-terphenyl by-product **6** was proposed by Power and co-workers during the preparation of the bulkier *m*-terphenyl phenols **2** and **3**, but was not observed because of the higher steric demands of his *m*-terphenyl backbone (11).

The structure of the nitrosobenzene compound **6** is interesting for two reasons. First of all, it confirms that the bulky Ar*Li can react with nitrobenzene either via oxygen atom abstraction or it can react via addition to nitrogen. Furthermore, the co-crystallized PhNO dimer was isolated in a rare *trans* configuration. Typically, PhNO does not dimerize, and when it does, it crystallizes in the *cis* form (22). Other structural parameters for both components of the red co-crystal are unremarkable, and no other unusual contacts were observed in the packing diagrams.

EPR of nitrobenzene complex 6

The EPR spectrum of a single co-crystal of complex **6** with homodimerized nitrosobenzene shows a single Lorentzian line with a relatively large peak-to-peak linewidth of 0.42 mT (Fig. 7, inset). This result is consistent with the presence of the paramagnetic nitroxide species,

Scheme 3. Synthesis of $[Me_2Al(\mu\text{-}OC_6H_3Mes_2)]_2$ **7**.

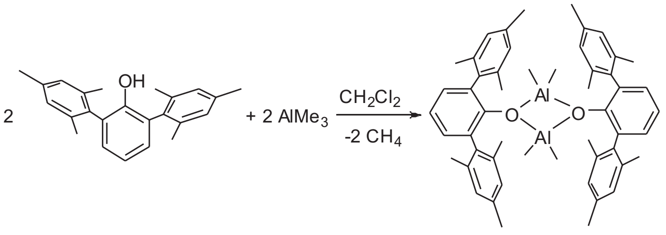

1 **7**

complex **6**; the broad, unresolved line is due to cross-relaxation between the spins of the radical species.

The crystal was dissolved in CH_2Cl_2 and a complex spectrum resulted, which was simulated accurately (Fig. 7, main panel). The magnitude and multiplicity of the hyperfine couplings are consistent with the structure of complex **6**. The large ^{14}N coupling ($I = 1$, $a(^{14}N) = 1.024$ mT) indicates that the majority of the spin density lies on the nitroxide moiety; couplings from a total of eight ^1H nuclei ($I = ½$, $a(^1H \times 3) = 0.247$ mT; $a(^1H \times 2) = 0.088$ mT, $a(^1H \times 3) = 0.054$ mT) demonstrate interactions with the eight protons of the phenyl groups directly attached to the nitroxide and indicate delocalization of spin density across both rings. The ^{14}N and ^1H hyperfine coupling constants measured for compound **6** are comparable to those observed for the symmetrical nitrosyl radical $C_6H_5N(O)C_6H_5$ (23).

Metal complexes derived from Ar*OH

The reaction of the *m*-terphenyl phenol **1** with an equimolar amount of $AlMe_3$ in dichloromethane gives the dialkylaluminium monophenoxide **7** (Scheme 3). Evidence for this product is found in the ^1H NMR spectrum, which showed peaks at –1.26, 2.15, and 2.19 ppm with relative intensities of 6:12:6, due to the aluminium methyls and *m*-terphenyl *ortho* and *para* methyl groups, respectively.

X-ray crystallographic studies (Fig. 8) confirmed the formula suggested by the ^1H NMR data, and showed that despite the bulk of the *m*-terphenyl ligand, **7** exists in the solid state as an oxygen-bridged dimer with a planar Al_2O_4 core. An identical motif was described by Rothwell for his less hindered 2,6-diphenylphenol aluminium complex (24). In contrast, Power's bulkier 2,6-bis(2,4,6-triisopropylphenyl)phenol aluminium complex was isolated as a base-stabilized monomeric ether solvate (25). As was the case in the free ligands, the effects of subtle steric differences around the *m*-terphenyl pocket have a remarkable effect on coordination within that pocket (Fig. 9).

To see if it was possible to establish a trend in the coordination behavior of the *m*-terphenyl phenols, group 14 derivatives were also prepared. Despite the fact that the first Sn(II) and Ge(II) compounds found to exist as dicoordinate monomers in the solid state were based upon bulky phenol ligands (26), structural data on divalent group 14 alkoxy or aryloxy compounds remains relatively rare. This makes the preparation of such compounds interesting simply from a fundamental perspective, but the fact that they are also being studied as catalysts (27) and as molecular precursors to superconductors and (or) ceramic materials for applications,

Fig. 8. Structure of $[Me_2Al(\mu\text{-}OC_6H_3Mes_2)]_2$ **7**. Thermal ellipsoids are shown at 50% probability, and hydrogen atoms and CH_2Cl_2 solvent have been removed for clarity. Selected bond lengths (Å): Al(1)—O(21) 1.8871(16); Al(1)—O(11) 1.8979(17); Al(2)—O(11) 1.8943(16); Al(2)—O(21) 1.9027(17); Al(1)—C(41) 1.942(3); Al(1)—C(42) 1.939(3); Al(2)—C(81) 1.942(3); Al(2)—C(82) 1.949(3); O(11)—C(11) 1.401(3); O(21)—C(51) 1.410(3). Selected bond angles (°): O(11)–Al(1)–O(21) 80.35(7); O(11)–Al(2)–O(21) 80.04(7); Al(1)–O(11)–Al(2) 99.54(7); Al(1)–O(21)–Al(2) 99.62(7).

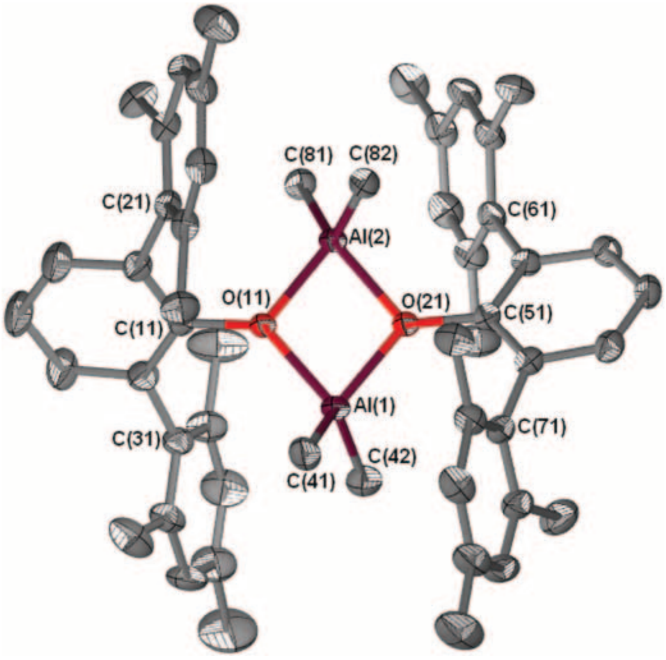

Fig. 9. Changes in the steric demands of the *m*-terphenyl backbone alter the coordination in the ligand binding pocket.

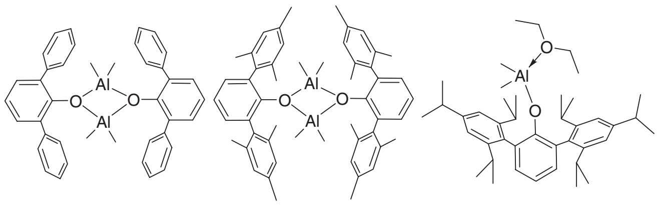

Ref. 24 **7** Ref. 25

Scheme 4. Synthesis of $[Sn(OC_6H_3Mes_2)_2]$ **8**.

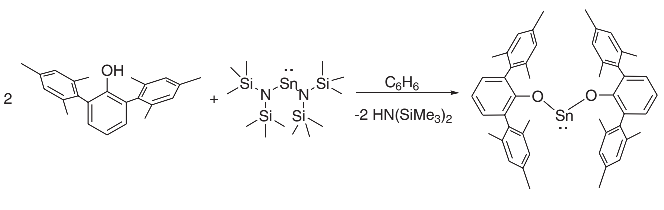

1 **8**

Fig. 10. Structure of [Sn(OC$_6$H$_3$Mes$_2$)$_2$] **8**, showing Sn–π interactions. Thermal ellipsoids are shown at 50% probability, and hydrogen atoms have been removed for clarity. Selected bond lengths (Å) and angles (°): Sn(1)—O(1) 2.039(3); Sn(1)—O(2) 2.043(3); O(1)—C(101) 1.343(5); O(2)—C(201) 1.342(5); O(1)–Sn(1)–O(2) 87.32(11); Sn(1)–O(1)–C(101) 127.7(2); Sn(1)–O(2)–C(201) 125.7(2).

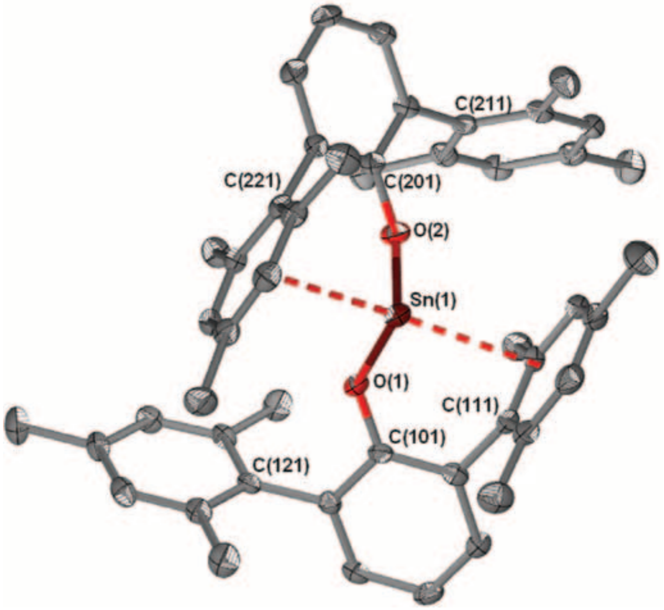

including flat panel displays, gas sensors, solar cells, and lithium battery anodes (28), makes structural data all the more important.

The protonolysis reaction (Scheme 4) of Sn[N(SiMe$_3$)$_2$]$_2$ with **1** in benzene gives the tin(II) complex **8** in good yield. No signal from the C*H*$_3$ groups of the trimethylsilylamide ligand was observed ^{1}H NMR spectrum of **8**, indicating that both amido groups had been lost to give the tin(II) bis(phenoxide) complex. The disappearance of the O*H* signal in both the ^{1}H NMR and IR spectra also indicated the formation of **8**, as did the peak at –344 ppm in the ^{119}Sn NMR spectrum. This value is upfield of the signal at –289 ppm for the most closely related Sn(OAr)$_2$ compound in the literature, namely Power's recently reported tin(II) bis(phenoxide) based on the *m*-terphenyl 2,6-bis(2,6-diisopropylphenyl)phenol **2** (25).

Final confirmation of the structure of **8** was provided by single-crystal X-ray diffraction. The crystallographic studies revealed that it does indeed exist as a monomer in the solid state (Fig. 10). The geometry at tin is v-shaped, due to the stereochemically active lone pair. As in the few other known monomeric Sn(II) bis(aryloxides) (25, 29), the O–Sn–O angle is quite acute, measuring only 87.32(11)°. The tin atom in **8** is not truly dicoordinate, however, as it has extensive Sn–π interactions resulting from being sandwiched between two flanking aryls of the *m*-terphenyl ligand. The Sn···centroid distances measure 2.942 and 2.980 Å for the C(111) and C(221) rings, respectively. Such interactions are also present in Sn(OAr)$_2$, where Ar = 2,6-bis(2,6-diisopropylphenyl) although they are somewhat longer [3.064 (C49 ring) and 3.262 (C7 ring)]. The observed upfield ^{119}Sn NMR shift for compound **8** may be due to the stronger Sn–arene interaction, but overall the interaction appears to be weak as shown by the appearance of only one set of signals for the *o*-Me protons in the ^{1}H NMR spectra of **8**.

Scheme 5. Synthesis of [(Me$_3$Si)$_2$NGe(OC$_6$H$_3$Mes$_2$)] **9** and Ge(OC$_6$H$_3$Mes$_2$)$_2$ **10**.

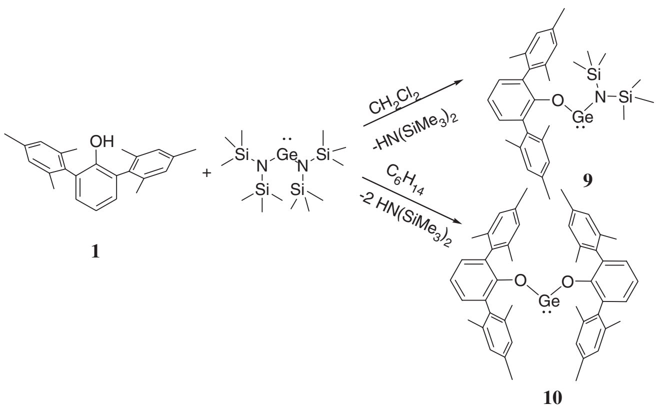

The reaction in dichloromethane of Ge[N(SiMe$_3$)$_2$]$_2$ with the *m*-terphenyl phenol **1** gave a mixture of compounds, one of which was the mixed aryloxy-amido germanium complex **9** (Scheme 5). This complex could be identified in the ^{1}H NMR spectrum of the crude reaction mixture as a singlet of 18 hydrogens at 0.00 ppm [–Si(C*H*$_3$)$_3$], and singlets at 2.18 and 2.42 ppm for the *ortho* and *para* methyls of the *m*-terphenyl ligand. Since Sn[N(SiMe$_3$)$_2$]$_2$ is known to react with dichloromethane solvent (3c, 30), it seemed possible that this could also be happening during the synthesis of **9**, so an attempt was made to repeat the synthesis in hexanes. Unfortunately, only traces of the mixed complex **9** were observed in the ^{1}H NMR spectrum. The major product was the germanium bis(aryloxide) **10**. As with the tin bis(aryloxide) **8**, the ^{1}H NMR spectrum of **10** showed a pronounced upfield shift of the *ortho* methyl protons to 1.79 ppm (1.82 ppm in **8**). Similarities were also seen in the elevated melting point of **10** at 318 °C, compared with 321 °C in **8**. Elemental analysis was consistent with the proposed composition of **10**.

Several attempts were made to grow crystals of **9** and **10**, but only **9** yielded single crystals suitable for X-ray diffraction studies (Fig. 11). Compound **9** is, to the best of our knowledge, the first structurally characterized monomeric, dicoordinate mixed aryloxy-amido germanium(II) complex (31). The Ge—O bond length of 1.8414(16) Å is longer than those found in other dicoordinate non-calixarene Ge(II) compounds [1.814(2) to 1.8296(14) Å] (25, 32). The opposite is true of the Ge—N bond, which, at 1.851(2) Å is shorter than in comparable compounds [1.855(2) to 1.939(6) Å] (33). The germanium atom does not engage in any significant inter- or intra-molecular interactions.

Given the interesting coordination patterns observed in the main-group complexes of **1**, we also wanted to probe its transition-metal coordination. For the related ligand 2,6-diphenylphenol, titanium complexes are by far the most common. Virtually, all of these complexes feature two *m*-terphenyl phenol ligands on the titanium centre, and a few even accommodate three (34). Only one complex is known with a single 2,6-diphenylphenol ligand, and it uses cyclo-

Fig. 11. Structure of $[(Me_3Si)_2NGe(OC_6H_3Mes_2)]$ **9**. Thermal ellipsoids are shown at 50% probability, and hydrogen atoms have been removed for clarity. Selected bond lengths (Å): Ge(1)—N(1) 1.851(2); Ge(1)—O(1) 1.8414(16); Si(1)—N(1) 1.753(2); Si(2)—N(1) 1.750(2); C(1)—O(1) 1.366(3). Selected bond angles (°): O(1)–Ge(1)–N(1) 97.59(8); Ge(1)–N(1)–Si(1) 122.83(11); Ge(1)–N(1)–Si(2) 114.71(11); Si(1)–N(1)–Si(2) 122.42(12).

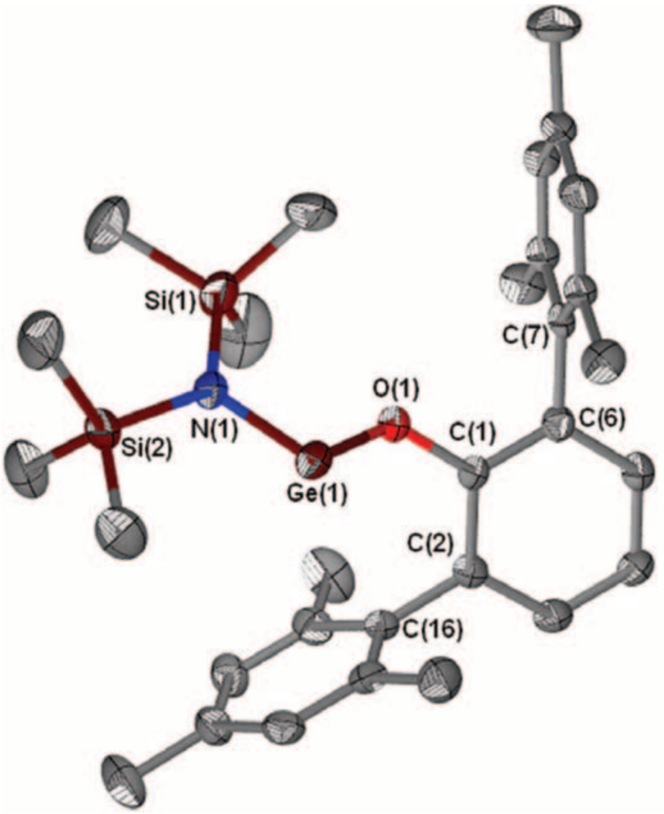

pentadienyl as an ancillary ligand (35). Would the increased bulk of **1** make it possible to isolate a titanium monophenoxide complex?

Addition of tetrakis(dimethylamino)titanium to a solution of **1** in dichloromethane resulted in the formation of an orange solid **11** (Scheme 6). The ^{1}H NMR spectrum showed a 1:1 ratio between the N*Me*$_2$ ligand at 2.30 ppm and the *m*-terphenyl at 2.24 (*para*) and 2.11 (*ortho*) ppm. Given that titanium is tetravalent, these data suggested the formation of a bis(phenoxide) complex with a formula of $(Me_2N)_2Ti(OC_6H_3Mes_2)_2$. This product was formed even when substoichiometric amounts of the *m*-terphenyl phenol ligand were added.

Scheme 6. Synthesis of $[(Me_2N)_2Ti(OC_6H_3Mes_2)_2]$ **11**.

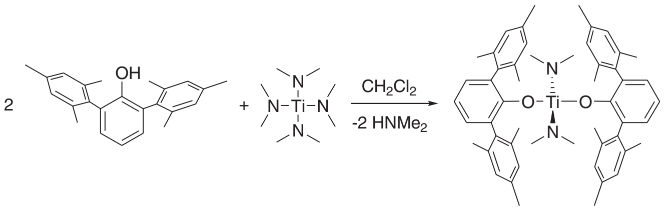

1 **11**

Fig. 12. Structure of $[(Me_2N)_2Ti(OC_6H_3Mes_2)_2]$ **11**. Thermal ellipsoids are shown at 50% probability, and hydrogen atoms have been removed for clarity. Selected bond lengths (Å): Ti(1)—N(31) 1.8822(13); Ti(1)—N(41) 1.8763(13); Ti(1)—O(11) 1.8460(10); Ti(1)—O(21) 1.8495(10). Selected bond angles (°): O(11)–Ti(1)–O(21) 119.25(5); O(11)–Ti(1)–N(41) 106.63(5); O(21)–Ti(1)–N(31) 107.72(5); O(21)–Ti(1)–N(41) 109.98(5); O(11)–Ti(1)–N(31) 109.17(5); N(31)–Ti(1)–N(41) 102.88(6).

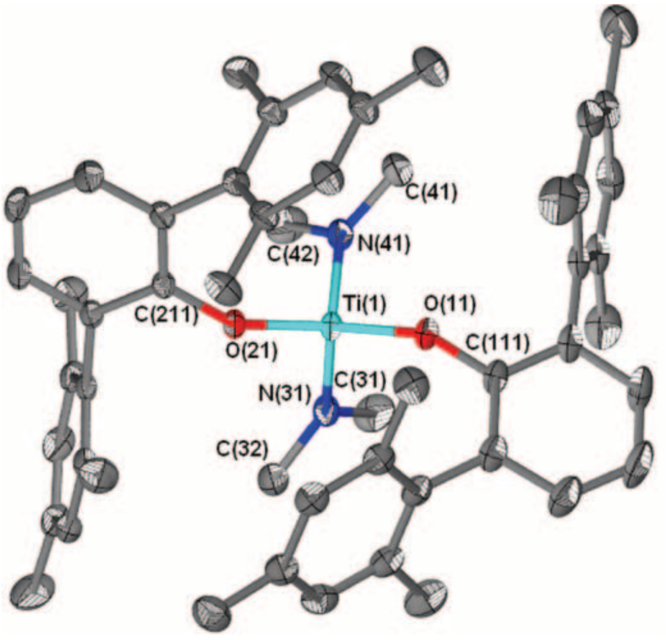

X-ray crystallographic studies of **11** confirmed the proposed structure (Fig. 12). The geometry at titanium is tetrahedral, with the greatest deviation in the O(11)–Ti(1)–O(21) angle [119.25.(5)°] and N(31)–Ti(1)–N(41) angle [102.88(6)°]. The Ti—O bonds are the same within experimental error, and are within the range of similar titanium complexes [1.786(2)–1.862(5) Å] (36). The same is true for the two Ti—N bond lengths, for which literature values of similar compounds range from 1.854(7) to 1.897(5) Å (36). The nature of the oxygen ligand appears to be the most-important factor governing the coordination at titanium. All but one of the structurally characterized examples of tetracoordinate titanium complexes with two oxygen donors and two nitrogen donors of any type, i.e., $[(R_2N)_2Ti(OR)_2]$, were based on 2,6-disubstituted phenol ligands. The one exception featured a 2,6-disubstituted aniline instead (37). It is not immediately clear if this is merely a coincidence or if the steric shielding of the *meta* substituents is chemically required.

Summary and conclusions

The X-ray crystal structures of a *m*-terphenyl phenol and a *m*-terphenyl boronic acid were described. The hydrogen bonding pattern observed in phenol **1**, intermolecular [O–H···O] dimerization, is very different from that observed in related *m*-terphenyl phenols. The steric demands of **1** are intermediate between those of previously characterized derivatives. This balance appears to be the key to the supramolecular interactions, as the same 2,4,6-trimethylphenyl substituent was used in the boronic acid **5** that also exhibited unprecedented [O–H···O] hydrogen bonds.

Given the differences in the structures of the free ligands, it seemed possible that the main-group and transition-metal complexes of **1** would also have features not found in more and (or) less bulky analogues. This was not the case for the titanium complex **11** and aluminium complex **7**. Both molecules were essentially isostructural to known 2,6-diphenylphenol derivatives. The tin complex **8**, on the other hand, did exhibit a spectroscopic difference. The secondary metal–π interaction between the tin atom and flanking aryls of the *m*-terphenyl ligand in **8** result in an up-field shift of the ^{119}Sn NMR resonance relative to that observed for $Sn(OAr)_2$, where Ar = 2,6-bis(2,6-diisopropylphenyl).

Experimental

General experimental

A nitrogen-atmosphere MBraun UL-99-245 dry box and standard Schlenk techniques on a double manifold vacuum line were used in the manipulation of air and moisture sensitive compounds. Solution-state NMR spectra were recorded in five millimetre tubes at Simon Fraser University on a Bruker AMX 400 or 600 MHz spectrometers or Varian AS 400 or 500 MHz spectrometers. Chemical shifts are reported in parts per million (ppm) downfield from $SiMe_4$ (^{1}H and ^{13}C), $BF_3{\cdot}Et_2O$ (^{11}B), or $SnMe_4$ (^{119}Sn). ^{1}H and ^{13}C spectra are calibrated to the residual signal of the solvent. ^{11}B and ^{119}Sn spectra are calibrated to the external $BF_3{\cdot}Et_2O$ or $SnMe_4$ standard. Infrared spectra were obtained using a Bomem MB spectrometer with the % transmittance values reported in cm^{-1}. EPR spectra were collected on a Bruker ECS-106 EPR spectrometer. The CH_2Cl_2 solution was deoxygenated by bubbling with nitrogen gas, to increase spectral resolution. Spectral simulation used the Bruker WinEPR SimFonia software. Melting points were measured using a Mel-Temp apparatus and are uncorrected. Elemental analyses were obtained at Simon Fraser University by Mr. M.K. Yang on a Carlo Erba Model 1106 CHN analyzer.

Anhydrous solvents were obtained from an MBraun Solvent Purification system, or were purchased from Aldrich and used without further purification. All other reagents and solvents were purchased from commercial sources, including Aldrich, Strem, and Gelest, and used without further purification, except deuterated solvents for NMR experiments on air- and (or) moisture-sensitive compounds, which were dried over P_2O_5 and distilled prior to use. The halogenated *m*-terphenyl precursors 2,4,6-triphenylbromobenzene (38) and 2,6-dimesityliodobenzene (39) were prepared according to literature procedures.

Synthesis of ligands and precursors

2,6-bis(2,4,6-Trimethylphenyl)phenol (1)

Under an inert atmosphere, *n*-BuLi (2.8 mL, 4.5 mmol, 1.6 mol/L in hexanes) was added dropwise to a suspension of 2,6-bis(2,4,6-trimethylphenyl)iodobenzene (1.32 g, 3.0 mmol) in 20 mL anhyd. Et_2O. After 2 h, the solution was cooled to –78 °C, and freshly distilled nitrobenzene (1.5 mL, 15 mmol) was added dropwise. The bright red solution was allowed to stir for 5 min, and then 20 mL of methanol was added slowly. After warming to RT, 30 mL of H_2O was added, and the organic layer was separated. The aq. layer was acidified with 1 mL concd. HCl and then extracted with Et_2O. The combined organic fractions were washed with water and saturated $NaCl_{(aq)}$ and then dried over $MgSO_4$. The solution was concentrated to ~10 mL and then passed through a plug of silica. After addition of ~10 mL pentane, the solution was left to evaporate slowly at room temperature overnight. The resultant pale brown solid was recrystallized to give colorless to pale blue crystals. Yield = 0.39 g (40%); mp = 145 °C. ^{1}H NMR ($CDCl_3$, 499.767 MHz,) δ: 7.03 (m, 3H), 6.98 (s, 4H), 4.53 (s, 1H), 2.33 (s, 6H), 2.06 (s, 12H). $^{13}C\{^1H\}$ NMR ($CDCl_3$, 100.624 MHz) δ: 137.5, 137.2, 135.9, 133.4, 129.6, 128.5, 128.1, 120.7, 21.2, 20.4. IR (nujol mull) ν: 3486 (s), 3451 (s), 1611 (w), 1584 (w), 1573 (w), 1490 (m), 1320 (s), 1260 (m), 1221 (vs), 1170 (s), 1089 (m), 1071 (m), 1030 (w), 1008 (w), 848 (vs), 829 (s), 797 (s), 780 (w), 752 (vs), 740 (w), 715 (w). Anal. calcd. for $C_{24}H_{26}O$: C, 87.23; H, 7.93. Found: C, 87.50; H, 8.04. HR-MS (*m/z*): [M$^+$] calculated for $C_{24}H_{26}O$, 330.198. Found: 330.198. During recrystallization small red single crystals of **6** can be isolated, a material that was identified as a co-crystal of $[C_6H_5N(O)]_2$ with $C_6H_5N(O)C_6H_3Mes_2$. The crystals can be isolated reproducibly in low yield (mg) per reaction. Mp = 120–123 °C. HR-MS $C_{30}H_{30}NO$ calcd.: 420.2327; found, 420.2315. IR (KBr pellet) ν: 2914 (s), 2857 (m), 1607 (m), 1573 (m), 1446 (vs), 1360 (m), 1307 (m), 1265 (m), 1221 (m), 1074 (m), 1024 (m), 846 (s), 753 (vs), 683 (s), 563 (m).

2,4,6-Triphenylphenylboronic acid (4)

Under an inert atmosphere, *n*-BuLi (9.7 mL, 1.6 mol/L in hexanes) was added to a suspension of 2,4,6-triphenylbromobenzene (5.00 g, 12.98 mmol) in 50 mL anhyd. Et_2O. After 2 h, the solution was cooled to –30 °C in a methanol/ice bath, and $B(OMe)_3$ (1.62 g, 15.57 mmol) was added dropwise. The reaction was warmed to RT and stirred overnight. The reaction was quenched with H_2O and allowed to stir 4 h before being extracted with Et_2O. The combined organic fractions were dried over $MgSO_4$, and then the solvent was removed under vacuum to give a pale yellow solid. Yield = 1.29 g (27%); mp = 356–357 °C. ^{1}H NMR ($CDCl_3$, 400.137 MHz) δ: 7.67 (d, 2H, *J* = 7.1 Hz), 7.63 (s, 2H), 7.53 (d, *J* = 6.8 Hz, 4H), 7.45 (t, *J* = 6.8 Hz, 6H), 7.40 (t, *J* = 7.1 Hz, 3H), 4.11 (s, 2H, $B(OH)_2$). $^{13}C\{^1H\}$ ($CDCl_3$, 125.679 MHz) δ: 146.8, 143.2, 142.1, 129.1, 128.8, 127.8, 127.5, 127.1, 126.9. ^{11}B ($CDCl_3$, 128.370 MHz) δ: 31.37. IR (nujol mull) ν: 3586 (vs), 3280 (br), 3056 (w), 3057 (w), 1595 (s), 1575 (w), 1538 (w), 1492 (s), 1445 (s), 1396 (s), 1335 (vs), 1208 (w), 1193 (w), 1083 (m), 1041 (m), 1030 (m), 983 (w), 917 (w), 888 (s), 821 (m), 782 (m), 761 (s), 751 (s), 699 (vs). Anal. calcd. for $C_{24}H_{19}BO_2$: C, 82.31; H, 5.47. Found: C, 82.62; H, 5.40.

2,6-bis(2,4,6-Trimethylphenyl)phenyl boronic acid (5)

Prepared according to the same procedure as **4**, beginning with 2,6-bis(2,4,6-trimethylphenyl)iodobenzene (5.0 g, 14.1 mmol). Yield = 3.67 g (73%); mp = 268–270 °C. ^{1}H NMR ($CDCl_3$, 400.137 MHz) δ: 7.53 (t, *J* = 7.5 Hz, 1H), 7.06 (d, *J* = 7.5 Hz, 2H), 6.99 (s, 4H), 4.06 (s, 2H), 2.33 (s, 6H), 2.02 (s, 12H). ^{13}C (CDCl$_3$, 125.679 MHz) δ: 146.9, 139.4, 137.8, 135.9, 130.9 (d), 129.1 (d), 128.6 (d), 21.4 (q), 20.8 (q). ^{11}B (CDCl$_3$, 128.370 MHz) δ: 29.30. IR (nujol mull) ν: 3668 (w), 3652 (w), 3646 (w), 3539 (br), 3417 (w), 1729 (w), 1613 (m), 1584 (m), 1561 (m), 1360 (s), 1309 (vs), 1261 (m), 1150 (w), 1112 (m), 1094 (m), 1087 (m), 1048 (m), 1038 (m), 848 (s), 811 (m), 759 (s), 742 (m), 666 (w), 656 (w). Anal. calcd. for $C_{24}H_{27}BO_2$: C, 80.46; H, 7.60. Found: C, 80.37; H, 7.49.

Synthesis of metal complexes

[Me$_2$Al(μ-OC$_6$H$_3$Mes$_2$)]$_2$ (7)

Under an inert atmosphere, AlMe$_3$ (1.01 mL, 2.0 mol/L in hexanes) was added dropwise to a solution of 2,6-bis(2,4,6-trimethylphenyl)phenol **1** (0.56 g, 1.69 mmol) in 10 mL anhyd. CH$_2$Cl$_2$. After stirring for 5 min at RT, the solution was concentrated under vacuum and then cooled to –30 °C. The next day, the solution was decanted from colorless crystals. Yield = 0.25 g (38%); mp = 238–240 °C. ^{1}H NMR (C$_6$D$_6$, 499.767 MHz) δ: 6.85 (s, 4H), 6.69 (t, J = 7 Hz, 1H), 6.59 (d, J = 7 Hz, 2H), 2.19 (s, 6H), 2.15 (s, 12H), –1.26 (s, 6H). ^{13}C NMR (C$_6$D$_6$, 125.680 MHz) δ: 138.3, 137.9, 135.9, 133.1, 129.5, 129.3, 128.3, 21.9, 21.7. IR (nujol mull) ν: 1610 (w), 1405 (m), 1261 (w), 1190 (m), 1182 (m), 1091 (m), 1032 (w), 848 (m), 825 (m), 803 (w), 774 (w), 758 (w), 701 (s), 635 (m). Anal. calcd. for$C_{52}H_{62}Al_2O_2$, C, 80.80; H, 8.08. Found: C, 81.14; H, 8.18.

[Sn(OC$_6$H$_3$Mes$_2$)$_2$] (8)

Under an inert atmosphere, a solution of Sn[N(SiMe$_3$)$_2$]$_2$ (0.33 g, 0.76 mmol) in 2 mL anhyd. benzene was added dropwise to a solution of 2,6-bis(2,4,6-trimethylphenyl)phenol **1** (0.50 g, 1.51 mmol) in 10 mL anhyd. benzene. The mixture was allowed to stir for 3 h at RT and then filtered. Slow evaporation of the solvent gave a yellow solid that was recrystallized from warm hexanes to give colorless crystals: Yield = 0.48 g (81%); mp = 321–322 °C. ^{1}H NMR (CD$_2$Cl$_2$, 499.767 MHz) δ: 6.84 (d, J = 6.9 Hz, 2H), 6.79 (s, 4H), 6.73 (t, J = 6.9 Hz, 1H), 2.29 (s, 6H), 1.82 (s, 12H). ^{13}C NMR (100.624 MHz, C$_6$D$_6$) δ: 157.8, 138.5, 137.8, 137.4, 129.7, 129.5, 129.2, 117.9, 21.1, 20.5. ^{119}Sn{^{1}H} (CD$_2$Cl$_2$, 223.867 MHz) δ: -344.23. IR (nujol mull) ν: 1610 (m), 1584 (m), 1412 (s), 1262 (m), 1246 (s), 1088 (w), 1072 (m), 1031 (br), 844 (vs), 798 (w), 787 (w), 752 (m), 739 (w), 649 (m). Anal. calcd. for $C_{48}H_{50}O_2Sn$: C, 74.14; H, 6.48. Found: C, 74.03; H, 6.39.

[(Me$_3$Si)$_2$NGe(OC$_6$H$_3$Mes$_2$)] (9)

Under an inert atmosphere, a solution of Ge[N(SiMe$_3$)$_2$]$_2$ (0.57 g, 1.45 mmol) in 2 mL CH$_2$Cl$_2$ was added dropwise to a solution of 2,6-bis(2,4,6-trimethylphenyl)phenol **1** (0.48 g, 1.45 mmol) in 5 mL anhyd. CH$_2$Cl$_2$. After 5 min, the solvent was removed under vacuum, and the crude product was recrystallized from benzene. Mp = 84–86 °C. ^{1}H NMR (C$_6$D$_6$, 499.768 MHz) δ: 7.62 (t, J = 7.5 Hz, 1H), 7.22 (d, J = 7.5 Hz, 2H), 7.03 (s, 4H), 2.42 (s, 6H), 2.18 (s, 12H), 0.00 (s, 18H). (This molecule was not isolated as an analytically pure compound).

[Ge(OC$_6$H$_3$Mes$_2$)$_2$] (10)

Under an inert atmosphere, a solution of Ge[N(SiMe$_3$)$_2$]$_2$ (0.24 g, 0.61 mmol) in 2 mL hexanes was added dropwise to a suspension of 2,6-bis(2,4,6-trimethylphenyl)phenol **1** (0.20 g, 0.61 mmol) in 5 mL anhyd. hexanes. After 45 min, the solvent was decanted from a white precipitate. Yield = 0.16 g (72%); mp = 318–319 °C. ^{1}H NMR (CD$_2$Cl$_2$, 499.767 MHz) δ: 6.81–6.88 (m, 3H), 6.75 (s, 4H), 2.29 (s, 6H), 1.79 (s, 12H). ^{13}C NMR (CD$_2$Cl$_2$, 125.678 MHz) δ: 138.1, 136.2, 129.5, 129.2, 128.8, 128.5, 119.2, 21.0, 20.1. IR (nujol mull) ν: 1610 (w), 1585 (w), 1484 (m), 1414 (s), 1260 (s), 1230 (vs), 1091 (m), 1071 (s), 1016 (m), 948 (w), 845 (vs), 799 (m), 754 (s), 739 (w), 728 (w), 670 (m), 659 (s), 609 (m). Anal. calcd. for $C_{48}H_{50}GeO_2$: C, 78.81; H, 6.89. Found: C, 79.14; H, 7.08.

[(Me$_2$N)$_2$Ti(OC$_6$H$_3$Mes$_2$)$_2$] (11)

Under an inert atmosphere, a solution of Ti(NMe$_2$)$_4$ (0.26 g, 1.15 mmol) in 5 mL anhyd. CH$_2$Cl$_2$ was added dropwise to a solution of 2,6-bis(2,4,6-trimethylphenyl)phenol **1** (0.76 g, 2.30 mmol) in 10 mL anhyd. CH$_2$Cl$_2$. The solution was allowed to stir for 10 min at RT and then cooled to –30 °C. After 3 h, the solution was decanted from orange crystals. Yield = 0.59 g (64%); mp 180 °C (dec.). ^{1}H NMR (C$_6$D$_6$, 400.137 MHz) δ: 6.82–6.87 (m, 7H), 2.30 (s, 6H), 2.24 (s, 6H), 2.11 (s, 12H). ^{13}C NMR (C$_6$D$_6$, 100.624 MHz) δ: 160.2, 137.3, 136.7, 135.6, 131.1, 130.5, 128.3, 120.2, 43.8, 21.0, 20.9. IR (nujol mull) ν: 3279 (m), 1611 (m), 1580 (m), 1484 (m), 1413 (vs), 1345 (m), 1251 (vs), 1229 (vs), 1146 (m), 1083 (s), 1054 (m), 1029 (m), 1008 (m), 950 (s), 904 (m), 876 (vs), 849 (vs), 799 (m), 778 (m), 757 (vs), 741 (w), 691 (vs), 679 (s), 597 (s). Anal. calcd. for $C_{52}H_{62}N_2O_2Ti$: C, 78.57; H, 7.86; N, 3.52. Found: C, 78.20; H, 7.83; N, 3.37.

Crystallographic studies[2]

The crystal was mounted on a glass fibre (**1**, **10**) or on the top of the nylon fibre of a CryoLoop™ (diameter of the nylon fibre: 10 microns (1 micron = 1 μm); loop diameter = 0.2–0.3 mm; Hampton Research, USA) (**5**–**8**, **11**). Data were collected at the temperature indicated in Table 1 on a Nonius Kappa-CCD diffractometer using monochromated Mo Kα radiation (λ = 0.71073 Å) with COLLECT (40). The unit-cell parameters were calculated and refined from the full data set. Crystal cell refinement and data reduction were carried out using DENZO (41). The data were scaled using SCALEPACK (41). The structures were solved by direct methods using SHELXTL-NT V6.1 suite of programs (42) (**1**, **6**, **8**, **10**) or SIR-97 (43) (**5**, **7**, **11**). All of the non-

---

[2] Supplementary data for this article are available on the journal Web site (canjchem.nrc.ca) or may be purchased from the Depository of Unpublished Data, Document Delivery, CISTI, National Research Council Canada, Ottawa, ON K1A 0R6, Canada. DUD 5242. For more information on obtaining material, refer to cisti-icist.nrc-cnrc.gc.ca/irm/unpub_e.shtml. CCDC 618683, 618675, 652069, 618680, 618685, 618681, and 618686 contain the crystallographic data for this manuscript. These data can be obtained, free of charge, via www.ccdc.cam.ac.uk/conts/retrieving.html (Or from the Cambridge Crystallographic Data Centre, 12 Union Road, Cambridge CB2 1EZ, UK; fax +44 1223 336033; or deposit@ccdc.cam.ac.uk).

Table 1. Crystallographic data for all crystallographically characterized compounds.

Crystal	**1**	**5**	**6**	**7**	**8**	**9**	**11**
Formula	$C_{24}H_{26}O$	$C_{24}H_{27}BO_2$	$C_{36}H_{35}N_2O_2$	$C_{52}H_{62}Al_2O_2$	$C_{48}H_{50}O_2Sn$	$C_{30}H_{43}GeNOSi_2$	$C_{52}H_{62}N_2O_2Ti$
FW	330.45	358.27	527.66	772.98	777.59	562.42	794.94
T [K]	173(2)	173(2)	173(2)	173(2)	173(2)	223(2)	173(2)
Color	Colorless	Colorless	Red	Colorless	Colorless	Pale yellow	Orange
Size	0.20 × 0.15 × 0.15	Not recorded	0.25 × 0.15 × 0.15	0.30 × 0.25 × 0.25	0.10 × 0.08 × 0.08	0.35 × 0.42 × 0.5	0.30 × 0.25 × 0.25
Cryst. syst.	Triclinic	Orthorhombic	Monoclinic	Monoclinic	Triclinic	Orthorhombic	Triclinic
Space group	P-1	$Cmc2(1)$	$P2_1/c$	$P2_1/c$	P-1	$P2(1)2(1)2(1)$	P-1
a [Å]	9.9380(2)	23.1780(3)	16.209(3)	17.5020(3)	9.7264(2)	11.6223(8)	10.96300(10)
b [Å]	11.5740(3)	12.9813(4)	11.417(2)	13.1600(3)	11.6250(3)	11.8066(8)	13.1040(2)
c [Å]	17.7140(6)	6.7470(6)	19.225(6)	22.3220(4)	18.1089(3)	23.2495(15)	16.5680(2)
a [°]	105.4600(13)	90	90	90	107.0250(10)	90	101.2510(5)
β [°]	100.3660(15)	90	125.3861(17)	109.5440(11)	90.2950(10)	90	98.8800(5)
γ [°]	94.5700(18)	90	90	90	90.8970(10)	90	99.5070(7)
V [Å^3]	1914.14(9)	2030.0(2)	2900.51(16)	4845.12(16)	1957.49(7)	3190.3(4)	2259.10(5)
Z	4	4	4	4	2	4	2
$D_{\text{calcd.}}$ [Mg m^{-3}]	1.147	1.172	1.208	1.060	1.319	1.171	1.169
μ [mm^{-1}]	0.068	0.072	0.074	0.096	0.690	1.056	0.230
$R_1{}^a$	0.0752	0.0464	0.0691	0.0581	0.0402	0.0280	0.0444
$wR_2{}^a$	0.2019	0.1141	0.1971	0.1713	0.1206	0.0698	0.1051
CCDC no.	618683	618675	652069	618680	618685	618681	618686

[a] $R_1 = [\Sigma||F_o| - |F_c||]/[\Sigma|F_o|]$ for $[F_o{}^2 > 2\sigma(F_o{}^2)]$; $wR_2 = \{[\Sigma w(F_o{}^2 - F_c{}^2)^2]/[\Sigma w(F_o{}^2)^2]\}^{1/2}$.

hydrogen atoms were refined with anisotropic thermal parameters. The hydrogen-atom positions were calculated geometrically and were included as riding on their respective heavy atoms. All figures were generated using X-SEED (44).

Due to the poor quality of the crystals for compound **5**, the quality of the data is rather low (parameter-to-reflection ratio is 1:6), and the bond distances and angles for the disordered BO_2 part and for the hydrogen bonding are not precise (rotational disorder of the oxygen atoms around the C–B bond). However, we believe that the molecular structure of **5** is correct. The Friedel pairs were averaged during the refinement, since this structure does not contain elements heavier than Si.

The crystal structure of compound **7** contains a severely disordered CH_2Cl_2 solvent molecule per asymmetric unit. Attempts to refine, applying a split-atom model, were unsuccessful. The data were corrected for the disordered electron density using the SQUEEZE (45) procedure as implemented in PLATON (46). A total solvent-accessible void volume of 539.5 Å^3 (11% of the unit-cell volume). Its contribution to the structure factors was ascertained using PLATON/SQUEEZE (35 e/unit cell). Derived values (formula weight, density, absorption coefficient) do not contain the contribution of the disordered solvent molecule

Acknowledgement

The authors thank Dr. Andrew Lewis (SFU) for collection of ^{11}B and ^{119}Sn NMR data, and Dr. Hilary Jenkins (SMU) for collection of X-ray crystallographic data. Funding was provided by the Canada Research Chairs Program, the Canadian Foundation for Innovation (CFI), the Natural Sciences and Engineering Research Council of Canada (NSERC), Simon Fraser University, and Saint Mary's University.

References

1. (*a*) B. Twamley, S.T. Haubrich, and P.P. Power. Adv. Organomet. Chem. **44**, 1 (1999); (*b*) J.A.C. Clyburne and N. McMullen. Coord. Chem. Rev. **210**, 73 (2000).
2. (*a*) D. Abeysekera, K.N. Robertson, T.S. Cameron, and J.A.C. Clyburne. Organometallics, **20**, 5532 (2001); (*b*) H.A. Jenkins, D. Abeysekera, D.A. Dickie, and J.A.C. Clyburne. J. Chem. Soc. Dalton Trans. 3919 (2002).
3. (*a*) D.A. Dickie, D.D. Choytun, M.C. Jennings, H.A. Jenkins, and J.A.C. Clyburne. Organomet. Chem. **689**, 2186 (2004); (*b*) D.A. Dickie, M.C. Jennings, H.A. Jenkins, and J.A.C. Clyburne. Inorg. Chem. **44**, 828 (2005); (*c*) D.A. Dickie, P.T.K. Lee, O.A. Labeodan, G. Schatte, N. Weinberg, A.R. Lewis, G.M. Bernard, R.E. Wasylishen, and J.A.C. Clyburne. Dalton Trans. 2862 (2007).
4. G.A. Horley, M.F. Mahon, K.C. Molloy, M.M. Venter, and P.W. Haycock, C.P. Myers. Inorg. Chem. **41**, 1652 (2002).
5. F. Quignard, M. Leconte, and J.-M. Basset. J. Chem. Soc., Chem. Commun. 1816 (1985).
6. (*a*) A.E. Fenwick, K. Phomphrai, M.G. Thorn, J.S. Vilardo, C.A. Trefun, B. Hanna, P.E. Fanwick, and I.P. Rothwell. Organometallics, **23**, 2146 (2004); (*b*) S.W. Schweiger, M.M. Salberg, A.L. Pulvirenti, E.E. Freeman, P.E. Fanwick, and I.P. Rothwell. J. Chem. Soc., Dalton Trans. 2020 (2004); (*c*) M.R. Lentz, J.S. Vilardo, M.A. Lockwood, P.E. Fanwick, and I.P. Rothwell. Organometallics, **23**, 329 (2004).
7. (*a*) J.R. Dilworth, J. Hanich, M. Krestel, J. Beck, and J. Strähle. Organomet. Chem. **315**, C9, (1986); (*b*) F. Quignard, M. Leconte, J.-M. Basset, L.-Y. Hsu, J.J. Alexander, and S.G. Shore. Inorg. Chem. **26**, 4272 (1987); (*c*) D.J. Darensbourg, B.L. Mueller, C.K. Bischoff, S.S. Chojnacki, and J.H. Reibenspies. Inorg. Chem. **30**, 2418 (1991); (*d*) R.K. Minhas, J.J.H. Edema, S. Gambarotta, and A. Meetsma. J. Am. Chem. Soc. **115**, 6710 (1993); (*e*) M.B. O'Donoghue, R.R. Schrock, A.M. LaPointe, and W.M. Davis. Organometallics, **15** 1334 (1996); (*f*) T. Hascall, M.-H. Baik, B.M. Bridgewater, J.H. Shin, D.G. Churchill, R.A. Friesner, and G. Parkin. Chem. Commun. 2644 (2002).
8. (*a*) A. Johansson and M. Håkansson. Chem. Eur. J. **11**, 5238 (2005); (*b*) T. Ooi, Y. Kondo, and K. Maruoka. Angew. Chem., Int. Ed. **37**, 3039 (1998).
9. (*a*) H. Ito, T. Nagahara, K. Ishihara, S. Saito, and H. Yamamoto. Angew. Chem., Int. Ed. **43**, 994 (2004); (*b*) S. Saito, T. Nagahara, M. Shiozawa, M. Nakadai, and H. Yamamoto. J. Am. Chem. Soc. **125**, 6200 (2003); (*c*) K. Maruoka, H. Imoto, S. Saito, and H. Yamamoto. J. Am. Chem. Soc. **116**, 4131 (1994).
10. (*a*) S. Saito and H. Yamamoto. Chem. Commun. 1585 (1997); (*b*) S. Saito, M. Shiozawa, T. Nagahara, M. Nakadai, and H. Yamamoto. J. Am. Chem. Soc. **122**, 7847 (2000).
11. C. Stanciu, M.M. Olmstead, A.D. Phillips, M. Stender, and P.P. Power. Eur. J. Inorg. Chem. 3495 (2003).
12. M. Niemeyer. Organometallics, **17**, 4649 (1998).
13. R.B. Bedford and M.E. Limmert. J. Org. Chem. **68**, 8669 (2003).
14. K.S. Webb and D. Levy. Tetrahedron Lett. **36**, 5117 (1995).
15. Y. Tokunaga, H. Ueno, Y. Shimomura, and T. Seo. Heterocycles, **5**7 787 (2002).
16. H. Nöth and B. Wrackmeyer. Nuclear magnetic resonance spectroscopy of Boron compounds. *In* NMR principles and progress. Vol. 14. *Edited by* P. Diehl, E. Fluck, and R. Kosfeld. Springer-Verlag, New York. 1978.
17. Cambridge Structural Database. Version 5.27. See: F.H. Allen. Acta Crystallogr. **B58**, 380 (2002).
18. (*a*) D.A. Dickie, A.Y.C. Chan, H. Jalali, H.A. Jenkins, H.-Z. Yu, and J.A.C. Clyburne. Chem. Commun. 2432 (2004); (*b*) D.A. Dickie, G. Schatte, M.C. Jennings, H.A. Jenkins, S.Y.L. Khoo, and J.A.C. Clyburne. Inorg. Chem. **45**, 1646 (2006).
19. M. Abbass, C. Kühl, C. Manthey, A. Müller, and U. Lüning. Collect. Czech. Chem. Commun. **69**, 1325 (2004).
20. K. Nakatsu, H. Yoshioka, K. Kunimoto, T. Kinugasa, and S. Ueji. Acta. Crystallogr., Sect. B. **34**, 2357 (1978).
21. V.E. Zavodnik, V.K. Belskii, and P.M. Zorkii. J. Struct. Chem. **28**, 793 (1987).
22. D.A. Dieterich, I.C. Paul, and D.Y. Curtin. J. Am. Chem. Soc. **96**, 6372 (1974).
23. P.H.H. Fisher and F.A Neugebauer. Z. Naturforsch, **19a**, 1514 (1964).
24. A.J.R. Son, M.G. Thorn, P.E. Fanwick, and I.P. Rothwell. Organometallics, **22**, 2318 (2003).
25. C. Stanciu, A.F. Richards, M. Stender, M.M. Olmstead, and P.P. Power. Polyhedron, **25**, 477 (2006).
26. B. Çetinkaya, I. Gümrükçü, M.F. Lappert, J.L. Atwood, R.D. Rogers, and M.J. Zaworotko. J. Am. Chem. Soc. **102**, 2088 (1980).
27. A. Kowalski, A. Duda, and S. Penczek. Macromolecules, **33**, 689 (2000).

28. (*a*) T.J. Boyle, J.M. Segall, T.M. Alam, M.A. Rodriguez, and J.M. Santana. J. Am. Chem. Soc. **124**, 6904 (2002); (*b*) T.J. Boyle, T.L. Ward, S.M. De'Angeli, H. Xu, and W.F. Hammetter. Chem. Mater. **15**, 765 (2003); (*c*) C.S. Weinert, P.E. Fanwick, and I.P. Rothwell. J. Chem. Soc., Dalton Trans. 1795 (2003).
29. D.M. Barnhart, D.L. Clark, and J.G. Watkin. Acta. Crystallogr., Sect. C **50**, 702 (1994).
30. M.F. Lappert, M.C. Misra, M. Onyszchuk, R.S. Rowe, and P.P. Power. J. Organomet. Chem. **330**, 31 (1987).
31. V.N. Khrustalev, I.A. Portnyagin, N.N. Zemlyansky, I.V. Borisova, M.S. Nechaev, Y.A. Ustynyuk, M.Y. Antipin, and V. Lunin. J. Organomet. Chem. **690**, 1172 (2005).
32. (*a*) C.S. Weinert, P.E. Fanwick, and I.P. Rothwell. J. Chem. Soc., Dalton Trans. 2948 (2002); (*b*) C.S. Weinert, A.E. Fenwick, P.E. Fenwick, and I.P. Rothwell. J. Chem. Soc., Dalton Trans. 532 (2003).
33. (*a*) R.W. Chorley, P.B. Hitchcock, M.F. Lappert, W.-P. Leung, P.P. Power, and M.M. Olmstead. Inorg. Chim. Acta, **198**, 203 (1992); (*b*) H. Braunschweig, P.B. Hitchcock, M.F. Lappert, and L.J.-M. Pierssens. Angew. Chem., Int. Ed. Engl. **33**, 1156 (1994); (*c*) M. Veith and A.Z. Rammo. Anorg. Allg. Chem. **627**, 662 (2001); (*d*) A. Meller, G. Ossig, W. Maringgele, M. Noltemeyer, D. Stalke, R. Herbst-Irmer, S. Freitag, and G.M. Sheldrick. Z. Naturforsch., Sect. B: Chem. Sci. **47**, 162 (1992). (*e*) C. Cui, M.M. Olmstead, J.C. Fettinger, G.H. Spikes, and P.P. Power. J. Am. Chem. Soc. **127**, 17530 (2005).
34. (*a*) R.W. Chesnut, L.D. Durfee, P.E. Fanwick, I.P. Rothwell, K. Folting, and J.C. Huffman. Polyhedron, **6**, 2019 (1987); (*b*) M.G. Thorn, Z.C. Etheridge, P.E. Fanwick, and I.P. Rothwell. J. Organomet. Chem. **591**, 148 (1999); (*c*) A. Sato, A. Hattori, K. Ishihara, S. Saito, and H. Yamamoto. Chem. Lett. **32**, 1006 (2003).
35. S.J. Sturla and S.L. Buchwald. Organometallics, **21**, 739 (2002).
36. (*a*) R.A. Jones, J.G. Hefner, and T.C. Wright. Polyhedron, **3**, 1121 (1984); (*b*) V.M. Visciglio, P.E. Fanwick, and I.P. Rothwell. Inorg. Chim. Acta, **211**, 203 (1993); (*c*) V.M. Visciglio. P.E. Fanwick, and I.P. Rothwell. Acta Crystallogr., Sect. C: Cryst. Struct. Commun. **50**, 896 (1994); (*d*) C.H. Zambrano, R.D. Profilet, J.E. Hill, P.E. Fanwick, and I.P. Rothwell. Polyhedron, **12**, 689 (1993).
37. J. Scholz, S. Kahlert, and H. Görls. Organometallics, **23**, 1594 (2004).
38. E.P. Kohler and L.W. Blanchard. J. Am. Chem. Soc. **57**, 367 (1935).
39. C.-J.F. Du, H. Hart, and K.K.D. Ng. J. Org. Chem. **51**, 3162 (1986).
40. B.V. Nonius. Kappa CCD Software [computer program]. Nonius BV, Delft, The Netherlands. 1999.
41. Z. Otwinowski and W. Minor. Processing of X-ray diffraction data collected in oscillation mode, methods in enzymology. *In* Macromolecular crystallography, Part A. *Edited by* C.W. Carter and R.M. Sweet. Academic Press. London. 1997. Vol. 276, pp. 307–326.
42. G.M. Sheldrick. SHELXTL NT V6.12, Program Library for Structure Solution and Molecular Graphics [computer program]. Bruker AXS, Inc. Madison, WI. 2000.
43. A. Altomare, G. Cascarano, C. Giacovazzo, A. Guagliardi, A.G.G. Moliterni, M.C. Burla, G. Polidori, M. Camalli, and R. Spagna. J. Appl. Crystallogr. **32**, 115 (1999).
44. (*a*) L.J. Barbour. J. Supramol. Chem. **1**, 189 (2001); (*b*) J.L. Atwood and L.J. Barbour. Cryst. Growth Des. **3**, 3 (2003).
45. P. van der Sluis and A.L. Spek. Acta Crystallogr. **46A**, 194 (1990).
46. A.L. Spek. PLATON: A multipurpose crystallographic tool [computer program]. Utrecht University, Utrecht, the Netherlands. 1998.